



UDP-4-Keto-6-Deoxyglucose, a Transient Antifungal Metabolite, Weakens the Fungal Cell Wall Partly by Inhibition of UDP-Galactopyranose Mutase

Liang Ma,^a Omar Salas,^b Kyle Bowler,^b Maor Bar-Peled,^{b,c} Amir Sharon^a

Department of Molecular Biology and Ecology of Plants, Tel Aviv University, Tel Aviv, Israel^a; Complex Carbohydrate Research Center, University of Georgia, Athens, Georgia, USA^b; Department of Plant Biology, University of Georgia, Athens, Georgia, USA^c

ABSTRACT Can accumulation of a normally transient metabolite affect fungal biology? UDP-4-keto-6-deoxyglucose (UDP-KDG) represents an intermediate stage in conversion of UDP-glucose to UDP-rhamnose. Normally, UDP-KDG is not detected in living cells, because it is quickly converted to UDP-rhamnose by the enzyme UDP-4-keto-6-deoxyglucose-3,5-epimerase/-4-reductase (ER). We previously found that deletion of the *er* gene in *Botrytis cinerea* resulted in accumulation of UDP-KDG to levels that were toxic to the fungus due to destabilization of the cell wall. Here we show that these negative effects are at least partly due to inhibition by UDP-KDG of the enzyme UDP-galactopyranose mutase (UGM), which reversibly converts UDP-galactopyranose (UDP-Galp) to UDP-galactofuranose (UDP-Galf). An enzymatic activity assay showed that UDP-KDG inhibits the *B. cinerea* UGM enzyme with a K_i of 221.9 μ M. Deletion of the *ugm* gene resulted in strains with weakened cell walls and phenotypes that were similar to those of the *er* deletion strain, which accumulates UDP-KDG. *Galf* residue levels were completely abolished in the Δ *ugm* strain and reduced in the Δ *er* strain, while overexpression of the *ugm* gene in the background of a Δ *er* strain restored *Galf* levels and alleviated the phenotypes. Collectively, our results show that the antifungal activity of UDP-KDG is due to inhibition of UGM and possibly other nucleotide sugar-modifying enzymes and that the rhamnose metabolic pathway serves as a shunt that prevents accumulation of UDP-KDG to toxic levels. These findings, together with the fact that there is no *Galf* in mammals, support the possibility of developing UDP-KDG or its derivatives as antifungal drugs.

IMPORTANCE Nucleotide sugars are donors for the sugars in fungal wall polymers. We showed that production of the minor sugar rhamnose is used primarily to neutralize the toxic intermediate compound UDP-KDG. This surprising finding highlights a completely new role for minor sugars and other secondary metabolites with undetermined function. Furthermore, the toxic potential of predicted transition metabolites that never accumulate in cells under natural conditions are highlighted. We demonstrate that UDP-KDG inhibits the UDP-galactopyranose mutase enzyme, thereby affecting production of *Galf*, which is one of the components of cell wall glycans. Given the structural similarity, UDP-KDG likely inhibits additional nucleotide sugar-utilizing enzymes, a hypothesis that is also supported by our findings. Our results suggest that UDP-KDG could serve as a template to develop antifungal drugs.

KEYWORDS *Botrytis cinerea*, UDP-4-keto-6-deoxyglucose, UDP-galactopyranose mutase, fungal cell wall, fungal nucleotide sugar metabolism, galactofuranose, metabolic intermediate

Received 28 August 2017 Accepted 13 October 2017 Published 21 November 2017

Citation Ma L, Salas O, Bowler K, Bar-Peled M, Sharon A. 2017. UDP-4-keto-6-deoxyglucose, a transient antifungal metabolite, weakens the fungal cell wall partly by inhibition of UDP-galactopyranose mutase. *mBio* 8:e01559-17. <https://doi.org/10.1128/mBio.01559-17>.

Editor Joseph Heitman, Duke University

Copyright © 2017 Ma et al. This is an open-access article distributed under the terms of the [Creative Commons Attribution 4.0 International license](https://creativecommons.org/licenses/by/4.0/).

Address correspondence to Maor Bar-Peled, peled@ccrc.uga.edu, or Amir Sharon, amirsh@ex.tau.ac.il.

The fungal cell wall is a robust yet flexible structure composed of different polysaccharide structures, including chitin, glucans, mannans, and a range of different proteins that are often glycosylated (1, 2). The cell wall is vital for fungal survival and proper development because it provides the fungal cell with mechanical strength, which contributes to the ability of the fungus to withstand osmotic changes and other stresses (3, 4). The vital role of the fungal wall and the absence of primary wall elements in mammals make the fungal wall a prime target for antifungal drugs. Indeed, several antifungal drugs target the wall, including polyoxins and echinocandins that target synthesis of chitin and beta-1,3-glucan, respectively (5).

The biosynthesis and remodeling of fungal cell walls involve concerted actions of enzymes that use a range of activated nucleotide sugars as donors to synthesize specific glycan components that are necessary for cell wall formation. For example, the synthesis of chitin is mediated by chitin synthases that utilize UDP-*N*-acetylglucosamine as a substrate to synthesize linear chitin (2), UDP-glucose is utilized by glucan synthases to produce various glucans (2), and GDP-mannose is used by mannosyltransferases to produce a range of proteins that are heavily decorated with mannose residues (manno-proteins) (6, 7). Other nucleotide sugars common in most fungi are UDP-galactopyranose (UDP-Galp) and UDP-galactofuranose (UDP-Galf), which are used for the synthesis of diverse types of polysaccharides (8) and glycoconjugates (9). In addition to the abundant sugars that are found in the cell walls of all fungal species, several types of minor UDP-sugars are found only in certain species, for example UDP-rhamnose (10, 11), UDP-xylose (12), and UDP-glucuronic acid (13).

Recently, two genes involved in the synthesis of UDP-4-keto-6-deoxyglucose (UDP-KDG) and UDP-rhamnose were identified (14) and analyzed in two plant-pathogenic fungi, *Botrytis cinerea* and *Verticillium dahliae* (10, 11). Deletion of the second gene (*er*) that encodes the enzyme UDP-4-keto-6-deoxyglucose-3,5-epimerase/-4-reductase (ER) resulted in accumulation of UDP-KDG and reduced the ability of both fungi to infect plants (10, 11). Interestingly, deletion of the *B. cinerea er* gene (*bcer*) also caused developmental defects that were associated with weakening of the cell wall; however, the mechanism leading to wall defects and reduced virulence remained unclear.

Many transporters and glycosyltransferases can accommodate multiple substrates and could be potentially inhibited by analogues of their nucleotide sugars (15–20). Given the structural similarity of UDP-KDG with many nucleotide sugars, we postulated that the toxicity of UDP-KDG might be due to inhibition of glycosyltransferases that utilize nucleotide sugars to assemble glycans and glycoconjugates. It is also possible that UDP-KDG affects enzymes that are involved in conversion of one nucleotide sugar to another. Accordingly, we searched for UDP-sugar-utilizing enzymes that could be putative targets of UDP-KDG. Here we report on the identification of the UDP-galactopyranose mutase (UGM) enzyme, which reversibly converts UDP-galactopyranose to UDP-galactofuranose, as a target of UDP-KDG. We show that UDP-KDG inhibits *B. cinerea* UGM, which results in reduced amounts of cellular and wall Galf, and weakening of the fungal cell wall.

RESULTS

Inhibition of UDP-galactopyranose mutase by UDP-KDG. A possible mechanism by which UDP-KDG affects cell wall integrity is inhibition of UDP-sugar-utilizing enzymes that are involved in the synthesis of other UDP-sugars like UDP-glucose, UDP-galactose (UDP-Gal), and UDP-*N*-acetylglucosamine. To test this possibility, we subjected the *Botrytis cinerea* genome to a BLAST search for homologues of proteins involved in nucleotide sugar metabolism. Among several candidate genes that were found, we selected BC1G_09363 (NCBI), which potentially encodes UDP-galactopyranose mutase (UGM), for further analysis. This gene was expressed in *Escherichia coli*, and enzymatic activity of the recombinant protein was determined. Figure S1 in the supplemental material shows that the BC1G_09363 protein is active as a UDP-galactopyranose mutase, transforming UDP-galactopyranose to UDP-galactofuranose in the presence of NADPH and flavin adenine dinucleotide (FAD) (Fig. S1C). This

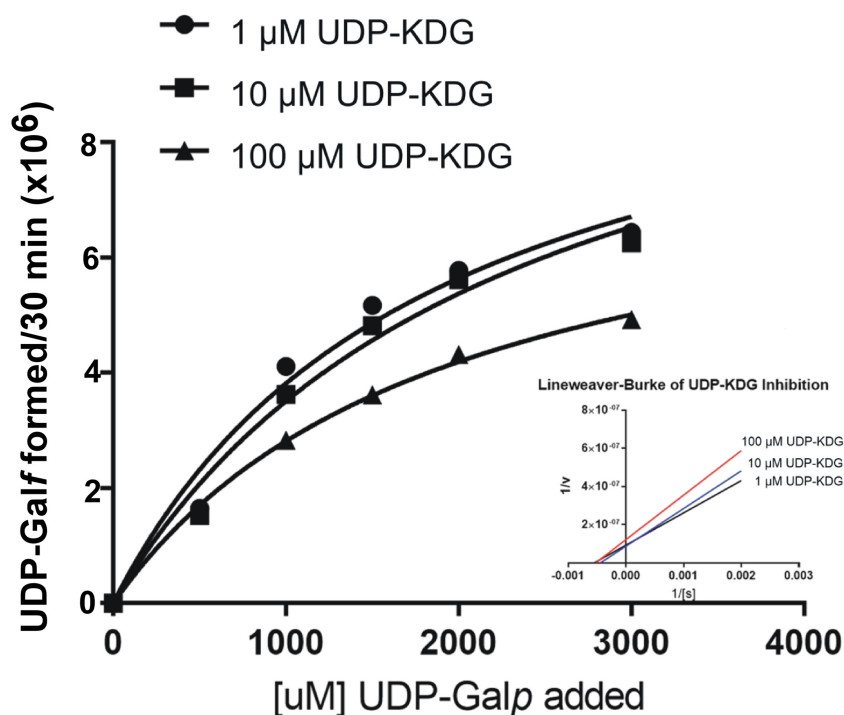


FIG 1 UDP-KDG inhibits *B. cinerea* UDP-galactopyranose mutase. Kinetic analyses were performed with increasing UDP-Galp concentrations (0.1, 0.5, 1.0, 1.5, 2.0, and 3.0 mM). For the inhibition assays, the reactions remained the same as for the kinetic analyses with the addition of various concentrations of UDP-KDG (1, 10, and 100 μ M).

interconversion catalysis was further determined by tandem mass spectrometry (MS/MS) analyses (Fig. S1G to I); hence, this gene product was named UDP-galactopyranose mutase. Kinetic analyses of enzyme activity showed that the K_m of the enzyme to UDP-Galp is 395 μ M and that it was strongly inhibited by UDP-KDG with a K_i value of 221.9 μ M (Fig. 1).

***bcugm* and *bcer* deletion strains share similar phenotypes.** To investigate whether the effects of UDP-KDG are mediated by inhibition of *B. cinerea* UGM (BcUGM), we generated *bcugm* deletion mutants and compared their phenotypes to those of a previously reported $\Delta bcer$ strain, which does not produce UDP-rhamnose but accumulates UDP-KDG (10). The following strains were used in the analyses: *bcugm* deletion strain $\Delta bcugm2b1$ (abbreviated Δugm) strain, *bcer* deletion strain $\Delta bcer9a2$ (abbreviated Δer) strain, *bcer bcugm* double deletion strain $\Delta bcer \Delta bcugm1c$ (abbreviated $\Delta er \Delta ugm$) strain, *bcugm* overexpression in the background of Δer strain $\Delta bcer::OEbcugm5a$ (abbreviated $\Delta er::OEUgm$) strain, and *bcugm* complementation strain $\Delta bcugm+bcugm6a$ (abbreviated $\Delta ugm+ugm$) strain.

(i) Mycelial growth. Colonies of the Δugm strain developed irregular mycelial clumps and had reduced radial growth rate compared with wild-type colonies (Fig. 2A and B). Both of these phenotypes were also observed in the Δer strain; however, they were more severe than in the Δugm strain, as demonstrated by more-intense formation of mycelial clumps and more-pronounced growth retardation. Furthermore, these phenotypes were even more severe in the $\Delta er \Delta ugm$ mutant strain, in which both the *bcer* and *bcugm* genes were deleted (Fig. 2A and B).

(ii) Sclerotium formation. After 11 days of incubation in dark, the Δugm strain produced aberrant sclerotia that were much smaller and less melanized than sclerotia produced by the wild-type strain (Fig. 2C). Similar to the growth-associated changes, the defects in sclerotium formation in the Δer strain were more pronounced than in the Δugm strain.

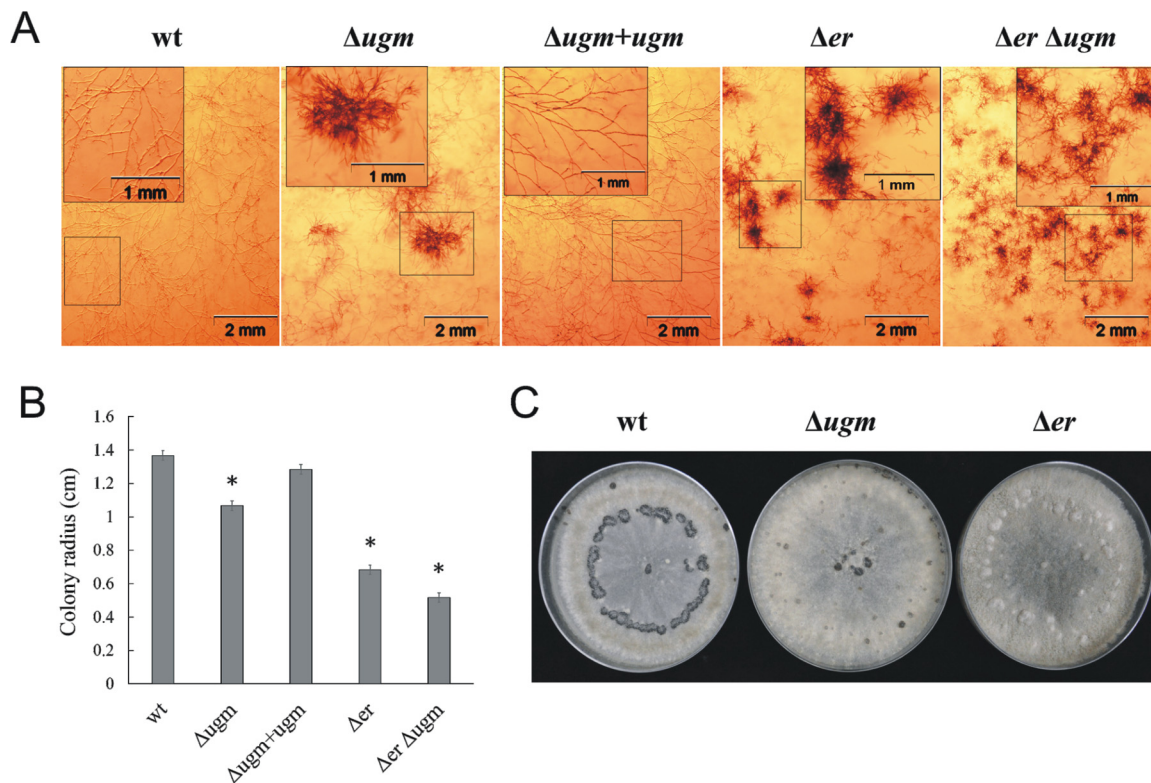


FIG 2 The $\Delta ug m$ strain and the Δer strain share similar developmental and growth abnormalities. Cultures were initiated by placing a 5- μ l droplet containing 500 spores in the center of each plate. (A) Fungi were cultured in CD medium under continuous light for 3 days. Cultures were inspected using a stereomicroscope, and images were captured. Photographs show hyphal organization of the wild-type (wt) strain, $\Delta ug m$ strain, $\Delta ug m + ug m$ complementation strain, Δer strain, and $\Delta er \Delta ug m$ double deletion strain. (B) Fungal growth in CD medium. Data are the mean radii plus standard deviations (SD) (error bars) for three 3-day-old colonies. Values that are statistically significantly different ($P < 0.01$ by two-tailed Student's t test) from the wild-type values are indicated by an asterisk. (C) Fungi were cultured on PDA medium in complete darkness for 11 days. Photographs show sclerotia formation of the wt, $\Delta ug m$, and Δer strains.

Pathogenicity. Infection of bean leaves with spores of the $\Delta ug m$ strain resulted in well-developed lesions at 3 days postinfection. These lesions were intermediate in size compared to the larger lesions of the leaves inoculated with the wild-type strain and the smaller lesions caused by the Δer strain (Fig. 3).

The similarity of the phenotypes for the $\Delta ug m$ and Δer strains supports the possibility that UDP-KDG inhibits BcUGM *in vivo*. The more-severe appearance of all of the

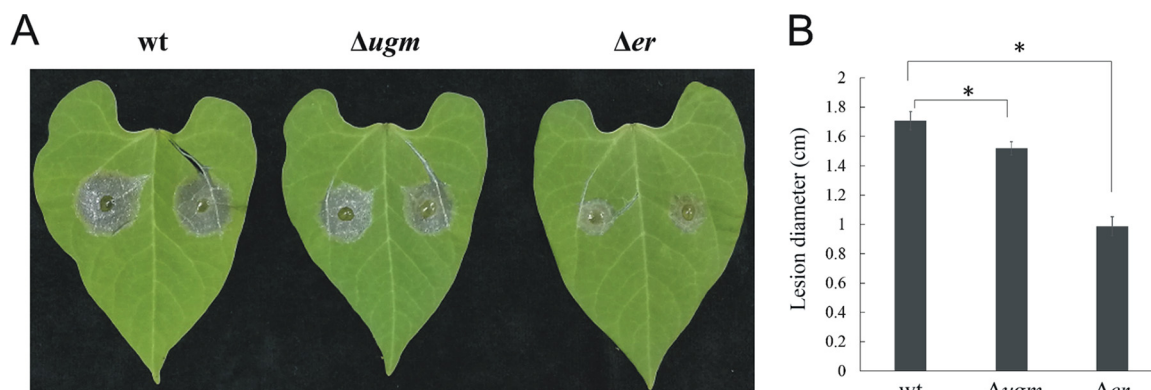


FIG 3 Mildly reduced virulence in the $\Delta ug m$ strain. Bean (*Phaseolus vulgaris*) leaves were inoculated with 7.5- μ l droplets of a spore suspension containing 10^5 spores/ml. Inoculated plants were incubated in a humid chamber at 22°C with light. (A) Typical lesions 3 dpi. (B) Average lesion size 3 dpi. Data are the means plus SD for eight lesions. Values that are statistically significantly different ($P < 0.01$) by two-tailed Student's t test from the wild-type values are indicated by a bracket and asterisk.

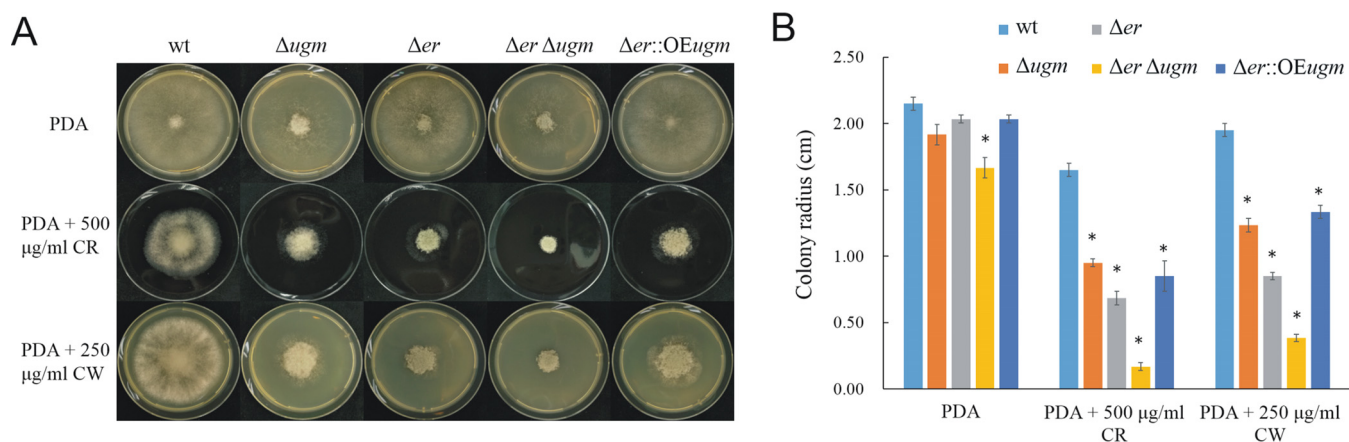


FIG 4 The Δ ugm strain displays cell wall defects. Colonies were initiated by placing a 5- μ l droplet containing 500 spores in the center of each plate, and the plates were incubated at 22°C. PDA plates contain 500 μ g/ml Congo red (CR) or 250 μ g/ml calcofluor white (CW) as cell wall stressors. (A) Colony spreading at 3 dpi. (B) Average colony radii measured at 3 dpi. Data are the mean radii \pm SD for three colonies. Values that are statistically significantly different ($P < 0.01$ by two-tailed Student's t test) from the wild-type values are indicated by an asterisk.

examined phenotypic characteristics in the Δ er strain indicates that UDP-KDG possibly has additional targets other than BcUGM, a hypothesis that is further supported by the even more severe phenotype of the Δ er Δ ugm double mutant.

The Δ ugm strain has cell wall defects. To test for possible alterations of the cell wall in the Δ ugm strain, fungi were cultured on media containing the cell wall stressors calcofluor white (CW) and Congo red (CR) that perturb cell wall assembly by binding to chitin (21, 22). Growth of the Δ ugm strain was markedly reduced on media containing either 500 μ g/ml CR or 250 μ g/ml CW, concentrations that only slightly inhibit growth of the wild-type strain (Fig. 4). These results show that the Δ ugm strain has a weakened cell wall, thus highlighting the importance of UGM for cell wall integrity. The effects of the cell wall stressors on growth of the Δ er or Δ er Δ ugm strains were even stronger than on growth of the Δ ugm strain, which is in accordance with the more-severe developmental defects observed in these strains. Overexpression of the *bcugm* gene in the Δ bcer background (Δ er::OEugm strain) partially compensated for the defects, further supporting the notion that UGM is inhibited by UDP-KDG in the Δ er strain (Fig. 4).

Caspofungin is an antifungal drug (a semisynthetic echinocandin) that inhibits the activity of (1 \rightarrow 3)- β -D-glucan synthase and thereby disturbs the integrity of the fungal cell wall (23). To test for possible synergism between inhibition of UGM and caspofungin, we cultured the strains on media and evaluated their sensitivity to caspofungin by using Etest strips (24). At 5 days postinoculation (dpi), the wild-type strain developed confluent growth in the presence of caspofungin and the MIC was 0.38 μ g/ml. The MIC for the Δ ugm strain was significantly less (0.047 μ g/ml), and a clear zone of inhibition was observed (Fig. 5). Similarly, the Δ er strain also showed a wider zone of inhibition compared to the wild type, with a caspofungin MIC (0.032 μ g/ml) lower than that of the Δ ugm strain (Fig. 5).

Collectively, these results provide evidence that loss or inhibition of BcUGM affects sensitivity of the fungus to cell wall-targeting compounds, confirming that the cell wall integrity of both strains is compromised.

Galactofuranose formation is inhibited in the Δ er strain. UGM enzymes catalyze the interconversion of UDP-Galp and UDP-Galf. Since UDP-Galf is the donor for Galf residues, comparison of Galf content in glycoproteins can be used to estimate the level of UDP-Galf. Consequently, if BcUGM is inhibited by UDP-KDG, the amount of the sugar residue Galf that is incorporated into cell wall glycans should be reduced in the Δ er strain. Fungal cell wall glycoproteins usually contain Galf in both N-linked glycans and O-linked glycans, which play important roles in protein stability, secretion, and localization (9). In order to determine the relative Galf content, we extracted both cell wall

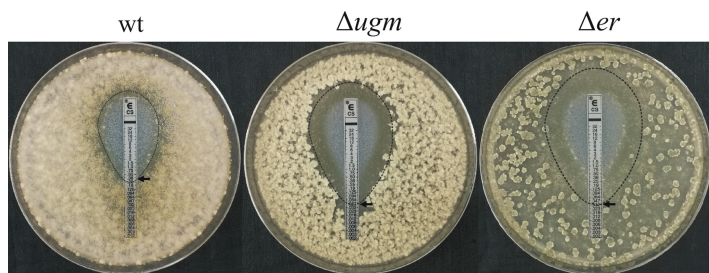


FIG 5 The Δugm and Δer strains are more susceptible to caspofungin. Etest strips impregnated with a gradient of caspofungin were placed on Gamborg-glucose agar plates containing 10^4 spores/ml of the different strains and cultured for 5 days at 22°C. The zone of inhibition is outlined by the black dashed line, and the MIC is read as the point where the ellipse of the zone of inhibition intercepts the test strip (black arrow).

proteins and total cellular proteins from different fungal strains and detected the Galf epitopes by Western blotting with anti-Galf monoclonal antibody L10-1 (25). Protein bands that mainly varied in size between 48 and 200 kDa were recognized in total cellular proteins and cell wall protein samples extracted from the wild-type strain (Fig. 6A and B). No signal was detected in samples of the Δugm strain, although equal amounts of proteins were loaded. The lack of antibody reaction with proteins extracted from the Δugm strain confirms the following. (i) The gene studied encodes a functional UGM. (ii) No alternative metabolic routes can form UDP-Galf. (iii) UDP-Galf is the sugar donor for the synthesis of Galf-containing glycoproteins in *B. cinerea*. Our working model suggests that UDP-KDG accumulation in the Δer strain has an inhibitory effect on

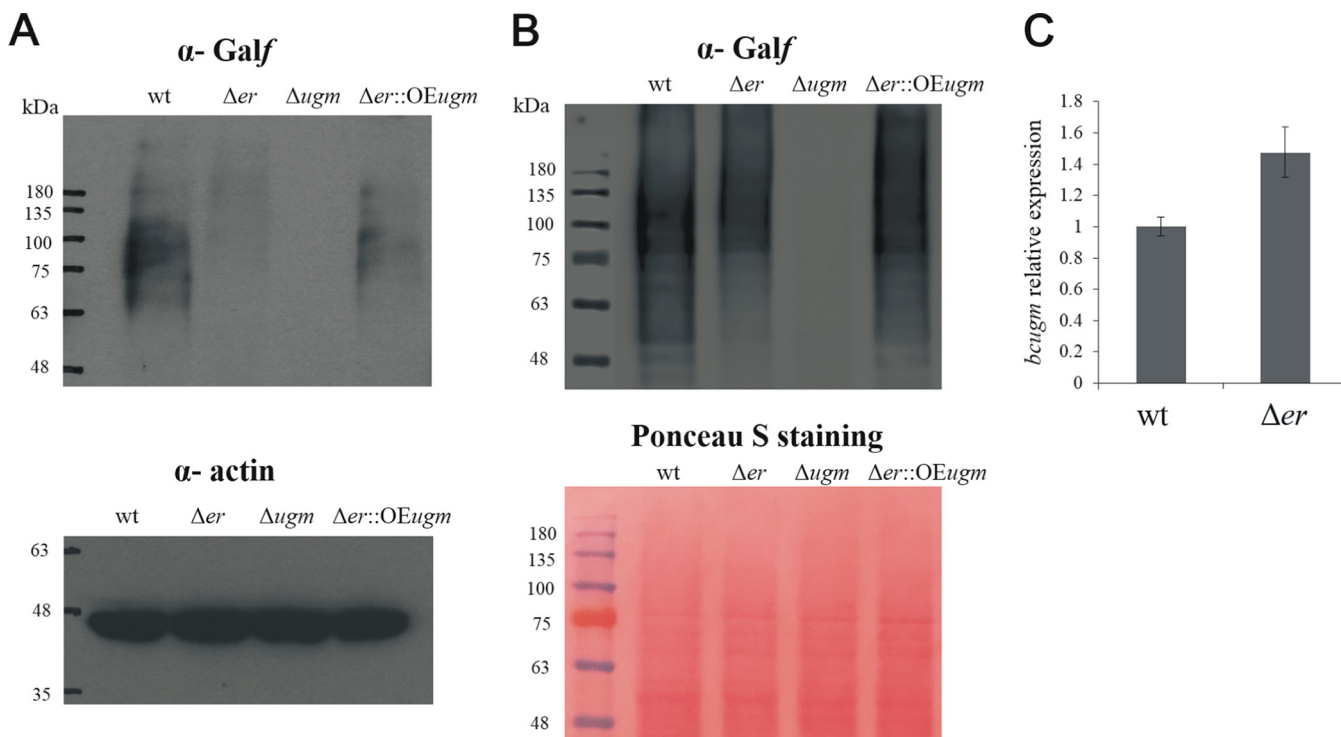


FIG 6 Galactofuranose (Galf) formation is reduced in the Δer strain. (A) Western blot to detect Galf content in total cellular proteins. One hundred micrograms of isolated proteins was loaded for each strain. (Top) Anti-Galf (α -Galf) L10-1 monoclonal antibodies were applied to detect Galf content. (Bottom) Antiactin monoclonal antibody was applied as a control for protein amount in total cellular protein samples. (B) Western blot to detect Galf content in cell wall proteins. Fifty micrograms of isolated proteins was loaded for each strain. (Top) Anti-Galf L10-1 monoclonal antibodies were applied to detect Galf content. Signals of samples on a single blot membrane were detected using a MicroChemi imaging system (DNR; Bio-Imaging Systems, Israel). The positions of molecular mass markers (in kilodaltons) of a merged protein ladder in the unlabeled leftmost lane are indicated to the left of the gel. (Bottom) The Ponceau S protein staining was used for a loading control. (C) Comparison of *bcugm* expression compared to *bcgpdh* expression.

overall formation of UDP-Galf. Accordingly, the Δer strain should contain reduced amounts of Galf in the glycoproteins. In agreement with this scenario, the anti-Galf signals in the Δer strain were significantly reduced in total cellular proteins (Fig. 6A) as well as in cell wall proteins (Fig. 6B) compared with the Galf amounts in protein extracts from the wild-type strain. Analysis of gene expression showed 1.5-fold-higher expression level of the *bcugm* gene in the Δer strain (Fig. 6C), ruling out the possibility that reduction of Galf level in glycoproteins is due to reduced levels of *bcugm* gene expression. Collectively, these results support our biochemical analyses that the reduced UGM enzymatic activity in the Δer strain results from inhibition of BcUGM by UDP-KDG.

DISCUSSION

Nucleotide sugars are precursors of primary metabolic pathways yielding diverse structures of glycoproteins, polysaccharides, and glycolipids (10). The fungal cell wall is composed primarily of glycans, including structural sugar polymers, such as chitin and glucans, and a range of glycoproteins that are decorated with various types of sugars. The roles of specific sugars within large polymers or glycoproteins are not easy to decipher, because the sugar may act as a structural element, it may act to stabilize an enzyme that is glycosylated, or it may have a role as a recognition epitope. In a previous study, we elucidated a two-step metabolic pathway of UDP-rhamnose production in *B. cinerea* (10). The first enzyme (UDP-glucose-4,6-dehydratase [DH]) converts UDP-glucose to produce the intermediate metabolite UDP-KDG, which is quickly converted to UDP-rhamnose by ER (see Fig. S2A in the supplemental material). A loss-of-function strain in which the entire UDP-rhamnose pathway was deleted was indistinguishable from the wild-type strain, and we could not infer any harmful consequence for the lack of rhamnose in the fungus. However, blocking of the second step of the pathway by deletion of the *bcer* gene led to multiple developmental defects, which were associated with weakening of the cell wall. We showed that the defects were due to accumulation of the intermediate metabolite UDP-KDG, which as far as we can tell is not used for metabolism other than UDP-rhamnose formation. Hence, the rhamnose metabolic pathway might serve as a shunt that prevents accumulation of UDP-KDG to toxic levels by converting it to UDP-rhamnose.

In humans, certain metabolic disorders are caused by the accumulation of toxic intermediate compounds when the product of an enzyme cannot be used by a downstream enzyme in the metabolic network (26). For example, classical galactosemia happens with infants who lack galactose-1-phosphate uridyl transferase activity (27), leading to the accumulation of galactose-1-phosphate, which functions as a potent competitive inhibitor of phosphoglucomutase to disrupt the glycolytic pathway (28). In microorganisms, accumulation of certain metabolic intermediates can also bring about toxic effects. For instance, accumulation of sugar-phosphates due to disruption of sugar metabolism have been shown to be highly toxic in *Mycobacterium tuberculosis* (29, 30). In the fungal system reported herein, deletion of *bcer* led to defects that result from accumulation of the toxic intermediate metabolite UDP-KDG, while lack of rhamnose had no effect on the fungus. Searching the JGI MycoCosm database (<http://genome.jgi.doe.gov/programs/fungi/index.jsf>) using *B. cinerea* DH (BcDH) as a query revealed that the 100 highest ranking fungi for blastp top hits also contained BcER homologues, further indicating that the *er* gene tends to coexist with the *dh* gene, probably as a safeguard to prevent accumulation of UDP-KDG.

Given the structural similarity of UDP-KDG with other nucleotide sugars, we reasoned that UDP-KDG might interfere with certain nucleotide sugar-utilizing enzymes. Among several potential targets, we found that UDP-KDG inhibits BcUGM. It is possible that the inhibition is due to the nature of UDP-KDG to exist in 4-hydrated form (Fig. S2B), but further studies, including cocrystallography of the BcUGM with UDP-KDG will be required to determine the nature of the interaction of BcUGM with UDP-KDG.

To evaluate whether inhibition of BcUGM by UDP-KDG is associated with the developmental defects of the Δer strain, we produced *bcugm* deletion strains and

compared their phenotypes with the phenotype of the Δer strain. Overall, the phenotypic characteristics of the Δugm strain resembled those of the Δer strain, including growth inhibition, developmental changes, impaired virulence, and weakening of the cell wall; however, the phenotypic changes of the Δugm strain were milder than those of the Δer strain. Coupled with *in vitro* inhibition of BcUGM by UDP-KDG, these results suggested that *in vivo* inhibition of BcUGM by UDP-KDG accounts at least partly for the developmental defects of the Δer strain. The consistently weaker effect in the Δugm strain suggests that UDP-KDG might have additional targets other than BcUGM. This possibility was further supported by the phenotypic characteristics of the $\Delta er \Delta ugm$ double deletion strain that were more severe than the phenotypic characteristics of the Δer strain and the milder phenotypic characteristics in the $\Delta er::OEugm$ double deletion mutant.

Since UGM facilitates the conversion of UDP-Galp to UDP-Galf, which is the donor for the Galf incorporated into glycans and glycoconjugates, the levels of Galf are indicative of UGM activity in the cell. We estimated the relative levels of Galf in the mutants by Western blot analysis using monoclonal antibodies that recognize Galf-containing epitopes. In accordance with the expected inhibition of BcUGM, Galf levels were markedly reduced (but not abolished) in the Δer strain. Transcript levels of the *bcugm* gene in the Δer strain were slightly higher than in the wild-type strain, further confirming that reduced Galf levels are due to inhibition of the BcUGM enzyme. In addition, Galf content in the $\Delta er::OEugm$ strain was higher than that in the Δer strain, indicating that the inhibition of Galf production by UDP-KDG can be mitigated by overexpressing *bcugm*. Taken together, these results show that UDP-KDG inhibits the enzymatic activity of BcUGM not only *in vitro* but also *in vivo*, resulting in decreased Galf levels and a weakening of the fungal cell wall.

Galf-containing structures are important for survival and pathogenicity in many pathogenic microorganisms. These Galf-containing structures include the lipopolysaccharides (LPS) O antigens of Gram-negative bacteria, extracellular or capsular polysaccharides of a variety of Gram-positive and Gram-negative bacteria, surface glycoconjugates of some protozoan parasites, as well as fungal cell wall and secreted molecules (8, 31). Because Galf production depends on UGM, changes or defects in UGM activity lead to changes in Galf that can affect fungal growth and virulence. For example, the *Aspergillus niger* Δugm mutant exhibits increased sensitivity to cell wall-perturbing agents (32), and in *Aspergillus nidulans*, the *ugm* gene is necessary for conidiation, hyphal growth, and morphogenesis, and it also affects antifungal drug sensitivity (33, 34). In addition, disruption of *ugm* in *Aspergillus fumigatus* results in weakened cell wall and likely attenuated virulence in mice (25, 35). Similarly, disruption of *bcugm* in *B. cinerea* resulted in weakened cell wall and other developmental defects. Since there is no Galf in mammals and higher plants, Galf biosynthetic pathways have been explored as attractive targets for the development of antibacterial drugs (36–41). The amino acid sequence conservation between prokaryotic and eukaryotic UGM is less than 15% (8), indicating that fungal and bacterial UGM enzymes are quite divergent. Because of these structural differences, it is expected that substrate binding mechanisms also differ in the fungal and bacterial UGM (42), and therefore, inhibitors of bacterial UGM are not expected to be efficient in fungi. Besides, all of these inhibitors were identified by *in vitro* enzymatic assays, which may not predict their entry into and true efficacy in living cells. Since UDP-KDG inhibits BcUGM both *in vitro* and *in vivo*, it might be possible to develop antimetabolites that mimic UDP-KDG as a UGM-targeting antifungal drug. Another way might be to identify compounds that inhibit nucleotide-rhamnose synthase (NRS)/ER enzyme as a way to force accumulation of toxic intermediates.

Although the Δugm strain phenocopied the Δer strain in various aspects, the phenotype differed in some specific features such as reduced spore size and delayed spore germination that were not observed in the Δer strain (Fig. S3). Considering the difference from the Δugm strain, the remaining low levels of Galf, or the specific salvage pathway stimulated by severe cell wall defects in the Δer strain, may underlie the

unique characteristics of the Δugm strain. On the other hand, the Δer strain displayed a more-debilitated phenotype than the Δugm strain did, meaning that BcUGM is not sufficient to account for all of the adverse effects brought about by UDP-KDG. In order to test whether UDP-KDG can inhibit other cell wall-synthesizing enzymes besides UGM, both *in vitro* and *in vivo* inhibition assays have yet to be performed.

Drug synergy can result when drugs target the same or functionally related pathway but through different targets (43). The higher sensitivity of the Δugm and Δer strains to cell wall inhibitors suggested that a UGM-targeting drug might be applied in combination with antifungal drugs that target other cell wall-synthesizing pathways, a notion that was supported by its potentiating the sensitivity of the mutants to caspofungin. Because caspofungin inhibits the enzyme 1,3- β -D-glucan synthase, the combination of deletion of *bcugm* with caspofungin resulted in a synergistic effect. Interestingly, despite partial inhibition of BcUGM in the Δer strain, the sensitivity of the Δer strain to caspofungin was slightly higher than that of the Δugm strain, possibly due to inhibition of multiple targets by UDP-KDG. These results demonstrate the antifungal activity of UDP-KDG, but more research will be necessary to determine the true potential of UDP-KDG as a lead molecule for antifungal therapies.

MATERIALS AND METHODS

Fungi and medium. *Botryotinia fuckeliana* (de Bary) Whetzel (= *Botrytis cinerea*) strain B05.10 and derived transgenic strains were cultured on potato dextrose agar (PDA) (Acumedia, Lansing, MI) at 22°C with continuous fluorescent light supplemented with near-UV light. Routine culture or growth assays were carried out in potato dextrose broth (PDB) (Acumedia, Lansing, MI), Czapek Dox (CD) medium (0.3% NaNO₃, 0.05% KCl, 0.05% MgSO₄ · 7H₂O, 0.001% FeSO₄ · 7H₂O, 0.1% K₂HPO₄ · 3H₂O, 2% sucrose [pH 7.3]), or GB medium (Gamborg B5 including vitamin mixture; Duchefa Biochemie, Haarlem, the Netherlands) supplemented with 2% glucose (GB5-Glc).

Cloning and expression of *bcugm*. Bacterial codon-optimized *B. cinerea* gene BC1G_09363 (potentially encodes UDP-galactopyranose mutase [BcUGM]) was synthesized (GenScript). For recombinant protein production, the gene was PCR amplified and cloned into pET28b-Tev expression plasmid (44). PCR amplification primers included an extra 15-nucleotide sequence at the 5' end with homology to the cloning site of the pET plasmid (see Table S1 for the sequences of all primers). Primers Galp Mutase PIPE S and Galp Mutase PIPE AS were used to amplify the *bcugm* gene. For the vector, primers ZL169 and KB_T7t were used to amplify the pET28b-TEV which when expressed gives a fusion protein with N-terminal six histidines followed by a tobacco etch virus (TEV) recognition amino acid sequence.

Escherichia coli Rosetta2(DE3)pLysS strains containing pET28b-TEV_BcUGM or pET28b-TEV_BcDH (a control plasmid) were cultured overnight at 37°C with shaking at 250 rpm in 5 ml LB medium supplemented with 50 μ g/ml kanamycin and 35 μ g/ml chloramphenicol. Each culture was transferred to a flask containing 250 ml LB medium supplemented with the same antibiotics, and the flasks were incubated (37°C, 250 rpm) until cell density reached an optical density at 600 nm (OD₆₀₀) of 0.6 to 0.8. Isopropyl- β -D-1-thiogalactopyranoside (IPTG) was added to a final concentration of 1 mM, and the cultures were grown for 20 h (18°C, 250 rpm). The cells were collected by centrifugation (6,000 \times g, 10 min at 4°C) and washed with 20 ml cold double-distilled water (DDW), and each cell pellet was resuspended in 10-ml cold lysis buffer (50 mM Tris-HCl [pH 7.5], 50 mM NaCl, 10% glycerol, 1 mM EDTA, 0.5 mM phenylmethylsulfonyl fluoride [PMSF], and 1 mM dithiothreitol [DTT]). The cells were lysed by sonication in ice-cold water using a Misonix S-4000 sonicator (Misonix, Inc., Farmingdale, NY) equipped with 1/8-in. microtip probe (12 cycles with 1 cycle consisting of a 20-s pulse at 30% amplitude and 30 s off). After sonication, the samples were centrifuged (6,000 \times g for 15 min at 4°C), and the supernatant was recovered and centrifuged again at 20,000 \times g for 30 min at 4°C. The resultant supernatant was subjected to Ni column purification using a Fast-Flow Ni²⁺-Sephacolumn (GE Healthcare) (2 ml of resin packed in a polypropylene column [1-cm inner diameter by 15 cm]). Recombinant proteins were eluted with elution buffer containing increased concentrations of imidazole (10 to 250 mM) and analyzed by measurement of their specific activity and by SDS-PAGE followed by Coomassie blue staining.

Enzyme activities and inhibition assay. Activity of recombinant BcUGM was tested in a 50- μ l reaction solution containing 50 mM Tris-HCl (pH 7.5), 1 mM NADPH, 1 mM flavin adenine dinucleotide (FAD), and 1 mM UDP-galactopyranose. The initial reactions were performed at 30°C for 1 h and then inactivated by 98°C for 5 min. An equal volume of chloroform was added, the tubes were centrifuged for 5 min at 14,000 \times g, and 30 μ l of the upper aqueous phase was removed and mixed with 57 μ l acetonitrile and 3 μ l of 0.5 M ammonium acetate (pH 4.35). A portion (25 μ l) of this mixture was used for hydrophilic interaction liquid chromatography (HILIC) by high-performance liquid chromatography with a UV detector (HPLC-UV) and another 25 μ l was analyzed by liquid chromatography coupled to tandem mass spectrometry (LC-MS/MS) (10). The amount of product formed was determined by HPLC-UV.

Triplicate BcUGM assays were performed for kinetic analyses with increasing UDP-Galp concentrations (0.1, 0.5, 1, 1.5, 2, and 3 mM). Reactions were carried out at 30°C for 30 min with 20 μ l purified BcUGM with a fixed amount of FAD, NADPH, and Tris-HCl (pH 7.5). The amount of UDP-Galp was analyzed by HPLC-UV and verified by liquid chromatography and mass spectrometry with electrospray ionization,

ion trap, and time of flight technologies (LC-MS-ESI-IT-TOF). Kinetics were calculated by fitting enzyme kinetic curves using the GraphPad Prism 7 software.

For the inhibition assays, the reaction mixtures remained the same as for the kinetic analyses with the addition of various concentrations of UDP-KDG (1, 10, and 100 μ M). To obtain UDP-KDG compound, a large-scale reaction was performed with *B. cinerea* UDP-glucose-4,6-dehydratase (BcDH) that converts UDP-glucose to UDP-KDG. This 1-ml reaction consisted of 50 mM Tris-HCl (pH 7.5), 1 mM UDP-glucose, 1 mM NAD⁺, and BcDH (14). The reaction was conducted for 2 h and heat inactivated, and the product was separated by HPLC-UV and verified by LC-MS-ESI-IT-TOF. Calculation of inhibition was performed using GraphPad Prism 7.

Generation of *B. cinerea* mutant strains. *B. cinerea* *ugm* homologue (*bcugm*) (GenBank accession number [XM_001551972](#)) was identified by a BLAST search with *Aspergillus fumigatus* UDP-galactopyranose mutase (GenBank accession number [AJ871145](#)). The NCBI *B. cinerea* B05.10 genome sequence (GenBank accession number [XM_001551972](#)) and flanking region was used to design primers (Table S1).

B. cinerea *bcugm* deletion strains (Δ *bcugm* strains) were generated by replacing the entire open reading frame (ORF) of the *bcugm* gene with a hygromycin resistance cassette consisting of an *Aspergillus nidulans* *oliC* promoter (*PoliC*), a hygromycin phosphotransferase gene (*hph*), and *bcacr* (*B. cinerea* enoyl-[acyl carrier protein] reductase terminator (*Tacr*) (45). A deletion cassette was generated by adding 500 bp each of the 5' and 3' flanking regions of the *bcugm* gene on either side of the *hph* cassette by overlap PCR (Fig. S4). A double deletion strain of the *bcer* and *bcugm* genes (Δ *bcer* Δ *bcugm* strain) was generated by deleting the *bcugm* ORF with a nourseothricin resistance cassette (*nr*) in the background of a Δ *bcer* strain (short for Δ *bcer9a2* strain as mentioned in reference 10). The *bcugm-nr* deletion construct was assembled in the same way as described for the *hph* deletion cassette (Fig. S5).

A *bcugm* overexpression construct was prepared by placing the *bcugm* ORF under the strong H2B promoter of *B. cinerea* (10) and flanked by an *nr* selection cassette. The *B. cinerea*-specific *bcniiA* sequence (46) was included as a homology region for integration of the construct (pNAH-*ugm*) to the *bcniiA* locus in the *B. cinerea* genome (Fig. S6). The plasmid was linearized with *Ap*I restriction enzyme and used to transform the *B. cinerea* Δ *er* strain to generate the Δ *bcer::OEbcugm* strain as described previously (10).

A *bcugm* complementation cassette was prepared by assembling three PCR fragments using a Gibson Assembly master mix kit (New England Biolabs). The three fragments include the *bcugm* gene with the upstream 500-bp region as the promoter and the downstream 340 bp as the terminator, the *PoliC-nr* cassette, and the *Tcel5a* (*B. cinerea* *cel5a*; GenBank accession number [AY618929.1](#)) termination signal (Fig. S7). This construct was transformed to a Δ *bcugm* strain to generate the *bcugm* complementation strain (Δ *bcugm*+*bcugm* strain).

Genetic transformation of *B. cinerea* with the different DNA constructs was performed as previously described (10). Colonies that developed on the selection media were transferred to separate plates. At least 10 isolates were obtained for each type of strain, and DNA was extracted from each colony and analyzed by PCR to verify integration of the construct at the desired locus. Homokaryotic strains were obtained by single-spore isolation using a Sporeplay dissection microscope (Singer Instruments, UK). Derived colonies were analyzed by PCR to verify that the strain is homokaryotic at the desired locus, and additional rounds of single spore isolation were performed in cases of impurity. At least four separate single-spore isolates were obtained for each strain.

Cell wall integrity assay. Spores from 9-day-old PDA cultures were collected using sterile DDW and filtered through two layers of Miracloth (Millipore, USA). The spores were then diluted to 10⁵ spores/ml, and 5 μ l of a spore suspension of each strain was applied to the center of a PDA plate without or with the specified concentration of cell wall-inhibiting compounds calcofluor white (CW) or Congo red (CR). The plates were incubated at 22°C, and the radius of each colony was measured 3 days postinoculation (dpi). Each experiment was repeated at least five times with three replications per treatment.

To measure the MIC of caspofungin, the filtered spores were mixed into 20 ml of 50°C GB5-Glc medium to a final concentration of 10⁴/ml and immediately poured in 9-cm-diameter petri plates. Next, the Etest strips (bioMérieux, France), containing a continuous caspofungin concentration gradient from 0.002 to 32 μ g/ml, were placed on the surface of the inoculated agar media and incubated at 22°C. The Etest MIC was defined as the drug concentration at which the border of the elliptical zone of complete inhibition intersected the scale on the antifungal test strip. Assays were repeated three times.

Pathogenicity assay. Pathogenicity assays were performed on the leaves of 10-day-old bean plants (*Phaseolus vulgaris* cv. Dwarf sugar) as previously described (47). Four leaves from two plants (two leaves per plant) were used for each treatment. Leaves were inoculated with 7.5- μ l droplets of spore suspension (10⁵ spores/ml in GB5-Glc), and the radius of lesions was recorded every 24 h. Experiments were repeated at least five times.

Isolation of fungal proteins. (i) Cell wall proteins. Spores were collected from 9-day-old PDA cultures, filtered through two layers of Miracloth, and then added to a 50-ml Erlenmeyer flask with 10 ml PDB to a final concentration of 10⁶ spores/ml. Samples were incubated on an orbital shaker with agitation at 180 rpm for 24 h. Then, samples were centrifuged at 3,000 \times *g* for 10 min, and the supernatant was removed. Mycelial pellets were washed sequentially with 20 ml of DDW, 20 ml of washing solution A (1 M NaCl, 25 mM EDTA, 1 mM PMSF), and 20 ml of lysis buffer (10 mM Tris-HCl [pH 7.4], 10 mM EDTA, 1 mM PMSF) to remove proteins present in the medium and proteins that are loosely connected with the hyphae. This sequential washing cycle was performed three times for each washing step, then the washed mycelial pellets were dried by lyophilization overnight, and the dried pellets were homogenized by repeated homogenization using a TissueLyser (Qiagen) operating at 30 Hz for 3 min each time until complete cell breakage.

Cell wall proteins were isolated by a previously reported procedure (48) with modifications. The broken cells were suspended in 1 ml of ice-cold lysis buffer, vortexed thoroughly, and centrifuged at $1,200 \times g$ at 4°C for 10 min, and then the supernatant was decanted carefully. The cell wall pellets were suspended and washed sequentially in 20 ml of wash solution B (5 mM EDTA, 1 mM PMSF), 20 ml of wash solution C (1 M NaCl, 5 mM EDTA, 1 mM PMSF), and 20 ml of wash solution D (50 mM Tris-HCl [pH 8.0], 10 mM EDTA, 1 mM PMSF), with centrifugation at $1,200 \times g$ at 4°C for 10 min between each washing step. This sequential washing cycle was repeated three times for each washing step, the supernatant was decanted, and the wet wall pellets were weighed. Washed wall pellets were suspended in extraction buffer (50 mM Tris-HCl [pH 8.0], 50 mM EDTA, 2% [wt/vol] SDS supplemented with 30 mM 2-mercaptoethanol) at a ratio of 5 ml of buffer per 1 g of tissue, and the samples were vortexed for 10 s, boiled for 10 min, and then centrifuged at $12,000 \times g$ for 10 min. The supernatant was retained and concentrated using Vivaspin 6 centrifugal concentrators (Sartorius, Germany) with 10-kDa molecular weight cutoff (MWCO) at $3,000 \times g$ for 60 min. After every round of concentration, phosphate-buffered saline (PBS) buffer was added to the concentrator (Vivaspin 6) to rinse and remove excessive interference agents for protein quantification. The process was repeated six times, and protein concentration was determined using the bicinchoninic acid protein assay kit (Sigma).

(ii) Total proteins. Mycelia were collected, and the entire mycelial biomass was washed following the same steps as described above. The wet mycelial pellets were weighed and lyophilized, and then the dried frozen mycelia were homogenized and suspended in extraction buffer (5 ml per 1 g [wet weight] of mycelia). Samples were boiled for 10 min and centrifuged at $12,000 \times g$ for 10 min, and the supernatant containing total proteins was collected and subjected to Vivaspin concentration and bicinchoninic acid quantification as mentioned above.

Western blot analysis. Equal amounts of protein extracts were mixed with 4× SDS protein sample buffer (40% glycerol, 240 mM Tris-HCl [pH 6.8], 8% SDS, 0.04% bromophenol blue, 5% beta-mercaptoethanol), denatured by boiling for 5 min, and then separated on SDS-10% PAGE. Then, the gel was blotted onto a 0.45- μ m nitrocellulose membrane (Bio-Rad Laboratories), using wet transfer buffer (25 mM Tris base, 190 mM glycine [pH 8.3]) at 100 V for 1 h. The membranes were stained briefly with 0.2% Ponceau S dye. The blots were incubated for 2 h in blocking solution containing both Tris-buffered saline with Tween 20 (TBST) (50 mM Tris-HCl [pH 7.5], 200 mM NaCl, 0.05% [vol/vol] Tween 20) and low-fat powdered milk reconstituted to 5% (wt/vol), and then incubated for 2 h at room temperature with culture supernatant of the hybridoma producing monoclonal antibodies L10-1 which is specific for galactofuranose epitopes (25) at a 1:5 dilution in blocking solution. Mouse antiactin monoclonal antibody (MAB1501; Chemicon) was used as a control and to determine protein amounts. The membranes were washed in TBST and then incubated for 1 h at room temperature with goat anti-mouse immunoglobulin G conjugated to horseradish peroxidase (Jackson ImmunoResearch, USA), diluted 1:2,000 in blocking solution. The membranes were washed four times for 5 min each time with TBST and then developed with 10 ml of enhanced chemiluminescence (ECL; Amersham) detection solutions for 1 min.

RNA extraction and quantitative real-time PCR. *B. cinerea* strains were cultured under the same growth condition used for the isolation of cell wall proteins, mycelia were harvested 24 h postinoculation (hpi) by filtration through Miracloth and immediately frozen in liquid nitrogen. For RNA extraction, frozen samples were crushed using a TissueLyser (Qiagen). Total RNA was then isolated using a NucleoSpin RNA plant kit (Macherey-Nagel), and residual DNA was digested with DNase I (Thermo Scientific). An aliquot (1 μ g) of RNA was used as the template for cDNA synthesis with oligo(dT) primer using RevertAid first-strand cDNA synthesis kit (Thermo Scientific). Expression levels of *bcugm* were determined by real-time quantitative PCR (qPCR) with primers 24/25 (Table S1) using SYBR Premix Ex Taq II (TaKaRa) in an Mx3000P real-time PCR apparatus (Stratagene). The *bcgpdh* (BC1G_05277, primers 26/27) was used as a control gene to normalize data. The experiments were repeated three times.

Spore germination assay. Spores from 9-day-old PDA cultures were collected in PDB, filtered through two layers of Miracloth, and diluted to 5×10^4 /ml, and 30 μ l of spore suspension was added to each well of a 24-well cell culture plate (SPL Life Sciences, South Korea). The plate was incubated at 22°C, and germination rates were determined at 2-h intervals using an inverted microscope (Olympus). Experiments included four replications with 50 ± 10 spores per sample. The experiments were repeated three times.

Statistical analyses. The statistical significance between means was tested by Student's *t* test (an asterisk indicates $P < 0.01$ by two-tailed *t* test). In all graphs, values are the mean values for at least three independent experiments, each with at least three replications per treatment.

SUPPLEMENTAL MATERIAL

Supplemental material for this article may be found at <https://doi.org/10.1128/mBio.01559-17>.

FIG S1, TIF file, 2.7 MB.

FIG S2, TIF file, 2.5 MB.

FIG S3, TIF file, 2.7 MB.

FIG S4, TIF file, 2.4 MB.

FIG S5, TIF file, 2.0 MB.

FIG S6, TIF file, 2.6 MB.

FIG S7, TIF file, 1.6 MB.

TABLE S1, DOCX file, 0.01 MB.

ACKNOWLEDGMENTS

We thank Frank Ebel at the University of Munich for the gift of L10-1 monoclonal anti-Galf antibodies.

This work was supported by BARD grant IS 4051-12.

REFERENCES

- Bowman SM, Free SJ. 2006. The structure and synthesis of the fungal cell wall. *Bioessays* 28:799–808. <https://doi.org/10.1002/bies.20441>.
- Free SJ. 2013. Fungal cell wall organization and biosynthesis. *Adv Genet* 81:33–82. <https://doi.org/10.1016/B978-0-12-407677-8.00002-6>.
- Adams DJ. 2004. Fungal cell wall chitinases and glucanases. *Microbiology* 150:2029–2035. <https://doi.org/10.1099/mic.0.26980-0>.
- Latgé JP. 2007. The cell wall: a carbohydrate armour for the fungal cell. *Mol Microbiol* 66:279–290. <https://doi.org/10.1111/j.1365-2958.2007.05872.x>.
- Georgopapadakou NH, Tkacz JS. 1995. The fungal cell wall as a drug target. *Trends Microbiol* 3:98–104. [https://doi.org/10.1016/S0966-842X\(00\)88890-3](https://doi.org/10.1016/S0966-842X(00)88890-3).
- Nakajima T, Ballou CE. 1975. Yeast manno-protein biosynthesis: solubilization and selective assay of four mannosyltransferases. *Proc Natl Acad Sci U S A* 72:3912–3916. <https://doi.org/10.1073/pnas.72.10.3912>.
- Mora-Montes HM, Ponce-Noyola P, Villagómez-Castro JC, Gow NA, Flores-Carreón A, López-Romero E. 2009. Protein glycosylation in *Candida*. *Future Microbiol* 4:1167–1183. <https://doi.org/10.2217/fmb.09.88>.
- Tefsen B, Ram AF, van Die I, Routier FH. 2012. Galactofuranose in eukaryotes: aspects of biosynthesis and functional impact. *Glycobiology* 22:456–469. <https://doi.org/10.1093/glycob/cwr144>.
- Deshpande N, Wilkins MR, Packer N, Nevalainen H. 2008. Protein glycosylation pathways in filamentous fungi. *Glycobiology* 18:626–637. <https://doi.org/10.1093/glycob/cwn044>.
- Ma L, Salas O, Bowler K, Oren-Young L, Bar-Peled M, Sharon A. 2017. Genetic alteration of UDP-rhamnose metabolism in *Botrytis cinerea* leads to the accumulation of UDP-KDG that adversely affects development and pathogenicity. *Mol Plant Pathol* 18:263–275. <https://doi.org/10.1111/mpp.12398>.
- Santhanam P, Boshoven JC, Salas O, Bowler K, Islam MT, Saber MK, van den Berg GC, Bar-Peled M, Thomma BP. 2017. Rhamnose synthase activity is required for pathogenicity of the vascular wilt fungus *Verticillium dahliae*. *Mol Plant Pathol* 18:347–362. <https://doi.org/10.1111/mpp.12401>.
- Park JN, Lee DJ, Kwon O, Oh DB, Bahn YS, Kang HA. 2012. Unraveling unique structure and biosynthesis pathway of N-linked glycans in human fungal pathogen *Cryptococcus neoformans* by glycomics analysis. *J Biol Chem* 287:19501–19515. <https://doi.org/10.1074/jbc.M112.354209>.
- Bar-Peled M, Griffith CL, Ory JJ, Doering TL. 2004. Biosynthesis of UDP-GlcA, a key metabolite for capsular polysaccharide synthesis in the pathogenic fungus *Cryptococcus neoformans*. *Biochem J* 381:131–136. <https://doi.org/10.1042/BJ20031075>.
- Martinez V, Ingwers M, Smith J, Glushka J, Yang T, Bar-Peled M. 2012. Biosynthesis of UDP-4-keto-6-deoxyglucose and UDP-rhamnose in pathogenic fungi *Magnaporthe grisea* and *Botryotinia fuckeliana*. *J Biol Chem* 287:879–892. <https://doi.org/10.1074/jbc.M111.287367>.
- Handford M, Rodriguez-Furlán C, Orellana A. 2006. Nucleotide-sugar transporters: structure, function and roles *in vivo*. *Braz J Med Biol Res* 39:1149–1158. <https://doi.org/10.1590/S0100-879X2006000900002>.
- Caffaro CE, Hirschberg CB, Berninsone PM. 2006. Independent and simultaneous translocation of two substrates by a nucleotide sugar transporter. *Proc Natl Acad Sci U S A* 103:16176–16181. <https://doi.org/10.1073/pnas.0608159103>.
- Ma X, Liu P, Yan H, Sun H, Liu X, Zhou F, Li L, Chen Y, Muthana MM, Chen X, Wang PG, Zhang L. 2013. Substrate specificity provides insights into the sugar donor recognition mechanism of O-GlcNAc transferase (OGT). *PLoS One* 8:e63452. <https://doi.org/10.1371/journal.pone.0063452>.
- Ikeda Y, Koyota S, Ihara H, Yamaguchi Y, Korekane H, Tsuda T, Sasai K, Taniguchi N. 2000. Kinetic basis for the donor nucleotide-sugar specificity of beta1, 4-N-acetylglucosaminyltransferase III. *J Biochem* 128:609–619. <https://doi.org/10.1093/oxfordjournals.jbchem.a022793>.
- Ihara H, Ikeda Y, Taniguchi N. 2006. Reaction mechanism and substrate specificity for nucleotide sugar of mammalian alpha1,6-fucosyltransferase—a large-scale preparation and characterization of recombinant human FUT8. *Glycobiology* 16:333–342. <https://doi.org/10.1093/glycob/cwj068>.
- Bar-Peled M, Griffith CL, Doering TL. 2001. Functional cloning and characterization of a UDP-glucuronic acid decarboxylase: the pathogenic fungus *Cryptococcus neoformans* elucidates UDP-xylose synthesis. *Proc Natl Acad Sci U S A* 98:12003–12008. <https://doi.org/10.1073/pnas.211229198>.
- Roncero C, Durán A. 1985. Effect of Calcofluor white and Congo red on fungal cell wall morphogenesis: *in vivo* activation of chitin polymerization. *J Bacteriol* 163:1180–1185.
- Ram AF, Klis FM. 2006. Identification of fungal cell wall mutants using susceptibility assays based on Calcofluor white and Congo red. *Nat Protoc* 1:2253–2256. <https://doi.org/10.1038/nprot.2006.397>.
- Letscher-Bru V, Herbrecht R. 2003. Caspofungin: the first representative of a new antifungal class. *J Antimicrob Chemother* 51:513–521. <https://doi.org/10.1093/jac/dkg117>.
- Desnos-Ollivier M, Dromer F, Dannaoui E. 2008. Detection of caspofungin resistance in *Candida* spp. by Etest. *J Clin Microbiol* 46:2389–2392. <https://doi.org/10.1128/JCM.00053-08>.
- Heesemann L, Kotz A, Echtenacher B, Broniszewska M, Routier F, Hoffmann P, Ebel F. 2011. Studies on galactofuranose-containing glycostructures of the pathogenic mold *Aspergillus fumigatus*. *Int J Med Microbiol* 301:523–530. <https://doi.org/10.1016/j.ijmm.2011.02.003>.
- McGary KL, Slot JC, Rokas A. 2013. Physical linkage of metabolic genes in fungi is an adaptation against the accumulation of toxic intermediate compounds. *Proc Natl Acad Sci U S A* 110:11481–11486. <https://doi.org/10.1073/pnas.1304461110>.
- Leslie ND. 2003. Insights into the pathogenesis of galactosemia. *Annu Rev Nutr* 23:59–80. <https://doi.org/10.1146/annurev.nutr.23.011702.073135>.
- de Jongh WA, Bro C, Ostergaard S, Regenbergh B, Olsson L, Nielsen J. 2008. The roles of galactitol, galactose-1-phosphate, and phosphoglucosyltransferase in galactose-induced toxicity in *Saccharomyces cerevisiae*. *Bio-technol Bioeng* 101:317–326. <https://doi.org/10.1002/bit.21890>.
- Phong WY, Lin W, Rao SP, Dick T, Alonso S, Pethe K. 2013. Characterization of phosphofructokinase activity in *Mycobacterium tuberculosis* reveals that a functional glycolytic carbon flow is necessary to limit the accumulation of toxic metabolic intermediates under hypoxia. *PLoS One* 8:e56037. <https://doi.org/10.1371/journal.pone.0056037>.
- Pethe K, Sequeira PC, Agarwalla S, Rhee K, Kuhlen K, Phong WY, Patel V, Beer D, Walker JR, Duraiswamy J, Jiricek J, Keller TH, Chatterjee A, Tan MP, Ujjini M, Rao SP, Camacho L, Bifani P, Mak PA, Ma I, Barnes SW, Chen Z, Plouffe D, Thayalan P, Ng SH, Au M, Lee BH, Tan BH, Ravindran S, Nanjundappa M, Lin X, Goh A, Lakshminarayana SB, Shoen C, Cynamon M, Kreiswirth B, Dartois V, Peters EC, Glynne R, Brenner S, Dick T. 2010. A chemical genetic screen in *Mycobacterium tuberculosis* identifies carbon-source-dependent growth inhibitors devoid of *in vivo* efficacy. *Nat Commun* 1:57. <https://doi.org/10.1038/ncomms1060>.
- Pedersen LL, Turco SJ. 2003. Galactofuranose metabolism: a potential target for antimicrobial chemotherapy. *Cell Mol Life Sci* 60:259–266. <https://doi.org/10.1007/s000180300021>.
- Damveld RA, Franken A, Arentshorst M, Punt PJ, Klis FM, van den Hondel CA, Ram AF. 2008. A novel screening method for cell wall mutants in *Aspergillus niger* identifies UDP-galactopyranose mutase as an important protein in fungal cell wall biosynthesis. *Genetics* 178:873–881. <https://doi.org/10.1534/genetics.107.073148>.
- El-Ganiny AM, Sanders DA, Kaminskyj SG. 2008. *Aspergillus nidulans* UDP-galactopyranose mutase, encoded by *ugmA* plays key roles in colony growth, hyphal morphogenesis, and conidiation. *Fungal Genet Biol* 45:1533–1542. <https://doi.org/10.1016/j.fgb.2008.09.008>.
- Alam MK, El-Ganiny AM, Afroz S, Sanders DA, Liu J, Kaminskyj SG. 2012. *Aspergillus nidulans* galactofuranose biosynthesis affects antifungal drug sensitivity. *Fungal Genet Biol* 49:1033–1043. <https://doi.org/10.1016/j.fgb.2012.08.010>.
- Schmalhorst PS, Krappmann S, Verweijen W, Rohde M, Müller M, Braus GH, Contreras R, Braun A, Bakker H, Routier FH. 2008. Contribution of

- galactofuranose to the virulence of the opportunistic pathogen *Aspergillus fumigatus*. *Eukaryot Cell* 7:1268–1277. <https://doi.org/10.1128/EC.00109-08>.
36. Soltero-Higgin M, Carlson EE, Phillips JH, Kiessling LL. 2004. Identification of inhibitors for UDP-galactopyranose mutase. *J Am Chem Soc* 126:10532–10533. <https://doi.org/10.1021/ja048017v>.
 37. Karunan Partha S, Sadeghi-Khomami A, Cren S, Robinson RI, Woodward S, Slowski K, Berast L, Zheng B, Thomas NR, Sanders DA. 2011. Identification of novel inhibitors of UDP-galactopyranose mutase by structure-based virtual screening. *Mol Inform* 30:873–883. <https://doi.org/10.1002/minf.201100085>.
 38. Scherman MS, Winans KA, Stern RJ, Jones V, Bertozzi CR, McNeil MR. 2003. Drug targeting *Mycobacterium tuberculosis* cell wall synthesis: development of a microtiter plate-based screen for UDP-galactopyranose mutase and identification of an inhibitor from a uridine-based library. *Antimicrob Agents Chemother* 47:378–382. <https://doi.org/10.1128/AAC.47.1.378-382.2003>.
 39. Dykhuizen EC, May JF, Tongpenyai A, Kiessling LL. 2008. Inhibitors of UDP-galactopyranose mutase thwart mycobacterial growth. *J Am Chem Soc* 130:6706–6707. <https://doi.org/10.1021/ja8018687>.
 40. Kuppala R, Borrelli S, Slowski K, Sanders DA, Ravindranathan Kartha KP, Pinto BM. 2015. Synthesis and biological evaluation of nonionic substrate mimics of UDP-Galp as candidate inhibitors of UDP galactopyranose mutase (UGM). *Bioorg Med Chem Lett* 25:1995–1997. <https://doi.org/10.1016/j.bmcl.2015.03.006>.
 41. El Bkassiny S, N'Go I, Sevrain CM, Tikad A, Vincent SP. 2014. Synthesis of a novel UDP-carbasugar as UDP-galactopyranose mutase inhibitor. *Org Lett* 16:2462–2465. <https://doi.org/10.1021/ol500848q>.
 42. Oppenheimer M, Poulin MB, Lowary TL, Helm RF, Sobrado P. 2010. Characterization of recombinant UDP-galactopyranose mutase from *Aspergillus fumigatus*. *Arch Biochem Biophys* 502:31–38. <https://doi.org/10.1016/j.abb.2010.06.035>.
 43. Cokol M, Chua HN, Tazan M, Mutlu B, Weinstein ZB, Suzuki Y, Nergiz ME, Costanzo M, Baryshnikova A, Giaever G, Nislow C, Myers CL, Andrews BJ, Boone C, Roth FP. 2011. Systematic exploration of synergistic drug pairs. *Mol Syst Biol* 7:544. <https://doi.org/10.1038/msb.2011.71>.
 44. Yang T, Bar-Peled L, Gebhart L, Lee SG, Bar-Peled M. 2009. Identification of galacturonic acid-1-phosphate kinase, a new member of the GHMP kinase superfamily in plants, and comparison with galactose-1-phosphate kinase. *J Biol Chem* 284:21526–21535. <https://doi.org/10.1074/jbc.M109.014761>.
 45. Minz Dub A, Kokkelink L, Tudzynski B, Tudzynski P, Sharon A. 2013. Involvement of *Botrytis cinerea* small GTPases BcRAS1 and BcRAC in differentiation, virulence, and the cell cycle. *Eukaryot Cell* 12:1609–1618. <https://doi.org/10.1128/EC.00160-13>.
 46. Schumacher J. 2012. Tools for *Botrytis cinerea*: new expression vectors make the gray mold fungus more accessible to cell biology approaches. *Fungal Genet Biol* 49:483–497. <https://doi.org/10.1016/j.fgb.2012.03.005>.
 47. Shlezinger N, Minz A, Gur Y, Hatam I, Dagdas YF, Talbot NJ, Sharon A. 2011. Anti-apoptotic machinery protects the necrotrophic fungus *Botrytis cinerea* from host-induced apoptotic-like cell death during plant infection. *PLoS Pathog* 7:e1002185. <https://doi.org/10.1371/journal.ppat.1002185>.
 48. Pitarch A, Nombela C, Gil C. 2008. Cell wall fractionation for yeast and fungal proteomics. *Methods Mol Biol* 425:217–239. https://doi.org/10.1007/978-1-60327-210-0_19.